Unusual Phase Behavior of End-Functionalized Polystyrene-*block*-poly(*n*-butyl methacrylate) Copolymer with Maleic Anhydride

Jin Kon Kim,* Myung Im Kim, Hye Jeong Kim, and Dong Hyun Lee

National Creative Research Center for Block Copolymer Self-Assembly, Department of Chemical Engineering and Polymer Research Institute, Pohang University of Science and Technology, Kyungbuk 790-784, Korea

Unyong Jeong*

Department of Materials Science and Engineering, Yonsei University, 134 Shinchon-dong, Seoul, Korea

Hiroshi Jinnai and Kazuya Suda

Department of Macromolecular Science and Engineering, Graduate School of Science and Engineering, Kyoto Institute of Technology, Sakyo-ku, Kyoto 606-8585, Japan

Received June 11, 2007; Revised Manuscript Received August 3, 2007

ABSTRACT: The effect of various end-functional groups on the phase behavior of polystyrene-*block*-poly(*n*-butyl methacrylate) copolymer (PS-*b*-PnBMA) was investigated by using small-angle X-ray scattering, conventional and 3-D transmission electron microscopy, rheology, and Fourier-transformed infrared spectroscopy. A PS-*b*-PnBMA with maleic anhydride (SBM66-MAH) exhibited an unexpected thermoreversible transition occurring at higher temperature than its disorder-to-order transition temperature. The transition was very fast and induced a large increase in shear modulus. However, the transition at higher temperature was not observed in other PS-*b*-PnBMAs with carboxylic acid, diester, and hydrogen end groups.

I. Introduction

Addition of functional groups to polymer chains has long been used in lubrication, reactive compatibilization, or surface modification.[1−3] It is generally considered that the addition to the end-functional group (X) to polymers does not change the phase behavior of polymer blends (A/B) or block copolymers (A-*b*-B), as long as the molecular weight of the mother polymer is much larger (approximately an order of 100) than that of X.[4−6] However, when the Flory interaction parameters (χ) between X and each polymer (χ_{XA} and χ_{XB}) are considerably larger than χ_{AB}, single addition of the functional group might significantly change phase behavior of the block copolymer. This is because the phase behavior is governed by χN in which N is the total number of statistical segments, and χN is not negligible for a very large χ even at a very small N ($\sim$1).

Some research groups investigated the effect of the end groups on phase behavior of block copolymers.[6,7] Choi and Han[6] found that the order-to-disorder transition (ODT) temperature of an end-functionalized polystyrene-*block*-polyisoprene-*block*-polystyrene with carboxylic acid (SIS-COOH) was marginally increased ($\sim$2 °C) compared with that of neat SIS. On the other hand, Schacht and Koberstein[8] showed that when the fluorosilane end group ($Si(CH_3)_2(CH_2)_2(CF_2)_5CH_3$) is attached to PS, the lower critical solution transition temperature of PS/poly(vinyl methyl ether) blend increases by $\sim$10 °C. These results indicate that χ_{F-S} (or χ_{F-VME}) is much larger than χ_{S-VME}, whereas the difference between χ_{COOH-S} (or χ_{COOH-I}) and χ_{S-I} is not prominent. Therefore, the significant change in the phase behavior by the addition of the end-functional group is expected when χ_{AB} is much smaller compared with χ_{XA} and χ_{XB}. This condition could be met for end-functionalized block copolymers or polymer blends with weak interaction.

Previously, we reported the phase transition temperature of symmetric PS-*block*-poly(*n*-butyl methacrylate) copolymer (PS-*b*-PnBMA) was greatly changed by the addition of end-functional groups to the end of PnBMA block.[9] It is noted that PS-*b*-PnBMA exhibits the lower disorder-to-order transition (LDOT).[10−12] The end groups used in ref 9 were diester (diE), diacid (diCOOH), and maleic anhydride (MAH). The end-functionalized PS-*b*-PnBMA copolymers also exhibited LDOT. Among three end-functional groups, the largest decrease in the LDOT was observed for end-functional PS-*b*-PnBMA with MAH (SBM66-MAH).[9] In this study, we investigated the effect of MAH groups on microdomains of SBM66-MAH by using small-angle X-ray scattering (SAXS), conventional and 3-D transmission electron microscopy (TEM and TEMT), rheology, and Fourier-transformed infrared spectroscopy. We found that the MAH end group induced another transition occurring at a temperature higher than the LDOT, resulting in a large increase in storage modulus (G') and a small reduction in the lattice domain spacing.

II. Experimental Section

A symmetric PS-*b*-PnBMA (SBM66, the total weight-average molecular weight of 66 000, the polydispersity of 1.03, and the weight fraction of PS = 0.50) was prepared by successive addition of styrene and *n*-butyl methacrylate at −78 °C by using *s*-BuLi.[9,13] The detail synthetic procedures for the addition of the functional groups of di-*tert*-butyl maleate (diE), carboxylic acid (COOH), and maleic anhydride (MAH) to the end of the PS-*b*-PnBMA chain are described in ref 9.

The rheological properties were monitored with an Advanced Rheometrics Expansion System (ARES: TI Instrument Co.). The

* To whom correspondence should be addressed. E-mail: jkkim@postech.ac.kr, ujeong@yonsei.ac.kr.

10.1021/ma0712899 CCC: $37.00
Published on Web 09/15/2007

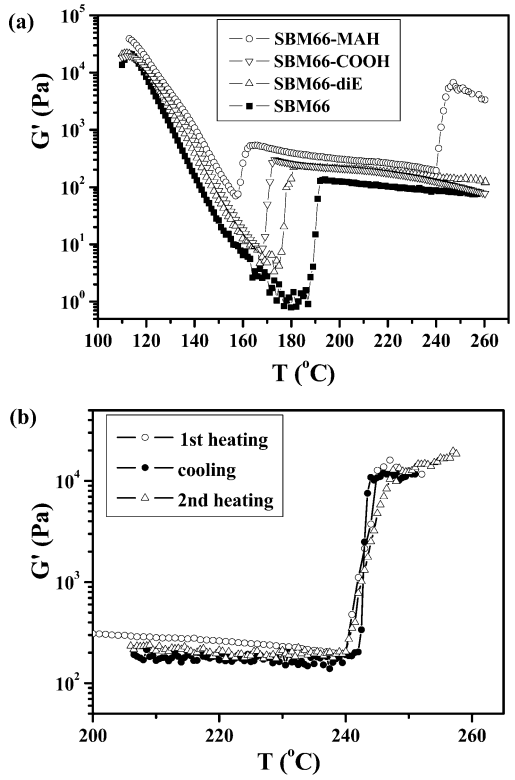

Figure 1. (a) Temporal changes of G' for PS-*b*-PnBMA (SBM66) and the end-functionalized derivatives with diester (SBM66-diE), carboxylic acid (SBM66-COOH), and maleic anhydride (SBM66-MAH). (b) Temporal change of G' of SBM66-MAH obtained during heating and cooling scans at a rate of 0.5 °C/min.

samples were compression-molded at 120 °C into disks (1.2 mm in thickness and 25 mm in diameter) and annealed at the same temperature for 10 h to remove the stress during the compression molding. The samples were first heated to 260 °C, cooled to 220 °C, and then reheated to 260 °C at a rate of 0.5 °C/min. Thermal degradation was not detected after the experiments, confirmed by size exclusion chromatography. The strain amplitude (γ_0) and the angular frequency (ω) were 0.05 and 0.1 rad/s, respectively, which lie in linear viscoelasticity.

Small-angle X-ray scattering (SAXS) profiles ($I(q)$ vs q ($= 4\pi \sin\theta/\lambda$), where q is the scattering vector and 2θ is the scattering angle) were conducted at the 4C1 beamline at the Pohang Light Source (PLS), Korea.[14] A one-dimensional position-sensitive detector (diode-array PSD; Princeton Instruments Inc.; model ST-120) with a distance of each diode of 25 μm was used. The sample thickness was 1.2 mm, and the sample-to-detector distance was 2.4 m. The exposure time was 2 min. All the samples were first annealed at 120 °C for 10 h, then heated to 270 °C, cooled to 220 °C, and finally reheated to 270 °C at a rate of 0.5 °C/min.

The structures of the microdomains were investigated with a transmission electron microscope (TEM; JEOL JEM-2200FS) operating at 200 kV. After being annealed at 120 °C for 10 h, one sample was heated to 230 °C at a rate of 0.5 °C/min and annealed for 3 h, followed by quenching into iced water. The other sample was heated to 260 °C at the same rate and annealed for 3 h and then also quenched from 260 °C. Ultrasectioning was performed with a microtomer (Reichelt ultracut UST, Leica Microsystems Inc., Germany) with a diamond knife at 25 °C. Finally, the specimens were stained with ruthenium tetroxide (RuO_4) vapor for 5 min at room temperature, which selectively stained the PS microdomains. These two TEM samples were also employed for 3D transmission electron microtomography (TEMT) to verify three-dimensional morphology. In the TEMT experiments, a series of TEM micrographs at different tilting angles were collected with a slow-scan CCD camera (Gatan USC1000, Gatan Inc.). To obtain achromatic projections, only the transmitted and elastically scattered electrons

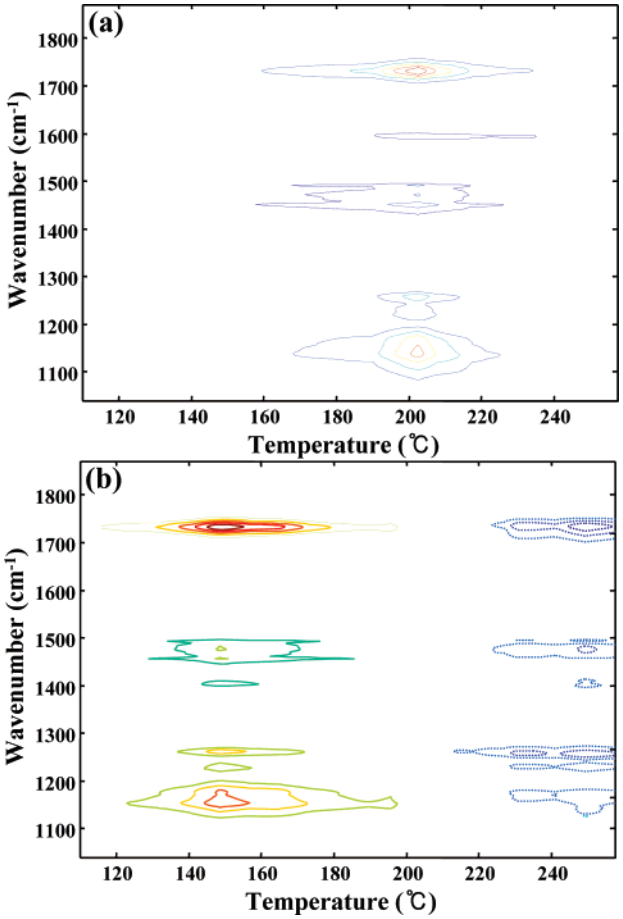

Figure 2. 2D maps of FTIR spectra of (a) SBM66 and (b) SBM66-MAH.

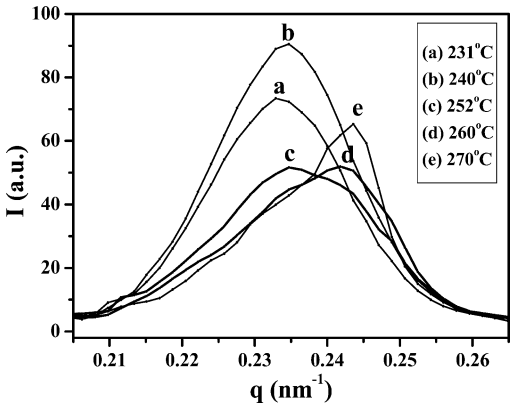

Figure 3. SAXS profiles for SBM66-MAH at various temperatures.

(electron energy loss: 0 ± 30 eV) were selected by an energy filter installed in the JEM-2200FS (Ω filter, JEOL Ltd., Japan).[15,16] The tilt series was taken over a tilt angle from 60° to −60° for the sample annealed at 230 °C and from 65° to −60° for the one annealed at 260 °C. The angular increment was 1° for both cases.

FTIR spectra were measured at a spectral resolution of 4 cm^{-1} with a Bomem DA8 FTIR spectrometer equipped with a liquid-nitrogen-cooled MCT detector. A Seagull attachment (Harrick Scientific Corp.), which includes a heating block attachment, was used in this study. A powder consisting of SBM66-MAH (or SBM66) and KBr was prepared by using a freezer mill. Before making the power, we annealed the block copolymer at 120 °C for 2 days to obtain the fully disordered state. All diffuse reflectance FTIR spectra were measured by coadding 256 scans from 100 to 270 °C at an interval of 5 °C after the sample was equilibrated for 30 min at the measurement temperature.

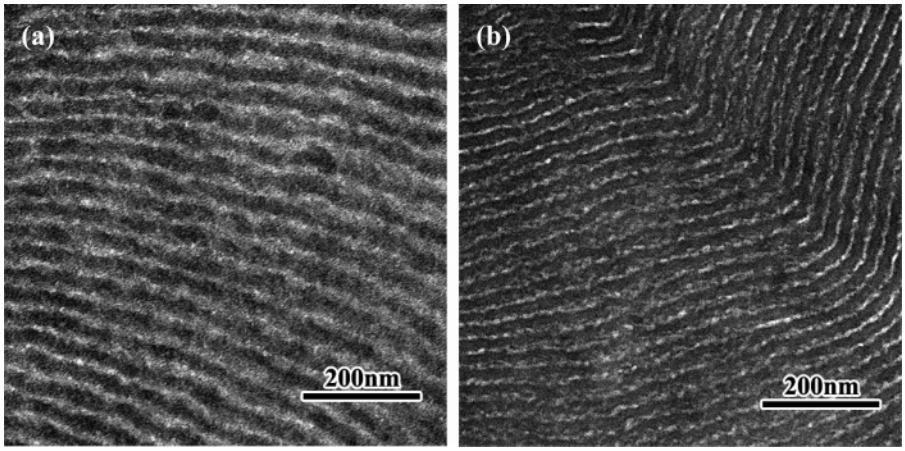

Figure 4. TEM images of SBM66-MAH prepared at (a) 230 °C for 3 h and (b) 260 °C for 3 h.

III. Results and Discussion

Temporal change in the storage modulus (G') is a useful means to monitor the transitions of a block copolymer.[17−19] In the previous study, we reported temporal changes in the storage modulus (G') of SBM66, SBM66-diE, SBM66-diCOOH, and SBM66-MAH up to 230 °C.[9] Addition of end-functional groups to SBM66 markedly decreased LDOT, even down to ca. 30 °C for SBM66-MAH. The surprising results were explained by the difference of interaction parameters ($\chi_{MAH-S} > \chi_{MAH-nBMA} \gg \chi_{S-nBMA}$). Figure 1a shows temporal changes in G' of the same block copolymers heated to 260 °C. All samples exhibited abrupt increase in G' at a critical temperature, which is referred to as LDOT. Very interestingly, SBM66-MAH exhibited another large jump in G' near 245 °C, whereas the other three block copolymers (SBM66, SBM66-diE, SBM66-diCOOH) did not. Such abrupt increase in G' for SBM66-MAH at high temperatures could be attributed to either a physical change of the morphology or a chemical change such as thermal cross-linking. Since SBM66-COOH and SBM66-diE did not show this behavior at high temperature, the increase in G' results from the existence of MAH groups at the chain ends. If chemical change or thermal cross-linking due to MAH groups occurs around 245 °C, the behavior of G' should be thermally irreversible. On the other hand, if the change of G' results from physical transition due to the morphological change, it should be thermally reversible. Figure 1b gives temporal change in G' during repeated heating and cooling scans. No thermal hysteresis was observed during the heating and cooling cycles, which indicates that the transition is induced by a physical change of the morphology.

The morphological transition is usually accompanied by the change of chain conformation. This could be monitored by Fourier-transformed infrared spectra. We recently showed that 2D map of FTIR detected the transition temperatures of block copolymers.[20,21] Parts a and b of Figure 2 give 2D maps of temperature-dependent FTIR of SBM66 and SBM66-MAH, respectively. The 2D map is a plot of dA/dT as a function of wavenumber and temperature (T), in which A is the absorption intensity.[22,23] It is seen that 2D map at all wavelengths for both SBM66 and SBM66-MAH exhibited the maximum at 200 and 150 °C, respectively. These temperatures correspond to their LDOTs. But, an additional maximum in the 2D map was observed at ca. 245 °C for SBM66-MAH, whereas it was not observed for neat SBM66. We further note that the additional maximum was not observed for SBM66-diE and SBM66-COOH, indicating the change of the chain conformation near 245 °C occurred in SBM66-MAH only.

Figure 3 gives SAXS profiles for SBM66-MAH at 230−270 °C. It is noted that only the first-order peak in SAXS profiles was observed due to the small electron contrast between PS and PnBMA. The peak intensity ($I(q^*)$) increased up to 240 °C during the heating, which is consistent with the nature of the LDOT behavior. Then, $I(q^*)$ decreased at 252 °C and increased gradually as the temperature was further raised. Interestingly, q^* at 260 (or 270 °C) was 0.245 nm^{-1}, ∼5% larger than that (0.233 nm^{-1}) at 240 °C, indicating that the domain spacing at higher temperatures was slightly, but not negligibly, smaller than that at lower temperature.

The morphological transition of SBM66-MAH near 245 °C was monitored with TEM images. Parts a and b of Figure 4 give TEM images of SBM66-MAH annealed at 230 and 260 °C for 3 h, respectively, followed by quenching into iced water. In contrast to the expectation from the results so far, these TEM images did not show any clear morphological change. They rather looked to have the same lamellar structures although some of microdomains at the higher temperature in Figure 4b exhibited disconnections and splitting along the microdomains. The domain spacing of a sample annealed at 260 °C appeared to be smaller than that annealed at 230 °C, which is consistent with SAXS profiles given in Figure 3. 3D-TEMT studies were also performed for the precise investigation of the morphology. The decrease of lamellar spacing of a sample annealed at 260 °C was also observed in the 3D-TEM cross-sectional images, but the morphological difference was not noticeable. (Full movies of 3D-TEMT images are given in the Supporting Information.)

The transition of SBM66-MAH at 245 °C was clearly demonstrated in Figures 1−3. Unfortunately, the weak contrast of electron density between PS and PnBMA led to a SAXS profile without having any higher order peaks, and TEM images could not clearly verify the change of the microdomains; thus, the detail change of microdomains during the transition could not be exactly explored. We might consider two possible reasons for the transition.

The first is that the transition might be due to the cluster formation between the end groups at high temperatures. The microphase separation between PS and PnBMA blocks may increase the number density of the end group in the central region of PnBMA microdomains. As the temperature is raised, the end groups become more concentrated because of the LDOT behavior between PS and PnBMA blocks. When the end groups have strong interaction between themselves, they might form small clusters in the central region of PnBMA microdomains. These clusters (or aggregations) might play as the physical cross-linking points for PnBMA chains and restrict severely the

motion of PnBMA chains; thus, a large G' would be expected. However, the MAH groups themselves do not have any strong interaction such as hydrogen bond. Rather, COOH end group should have higher possibility of the cluster formation arising from the hydrogen bonding compared with the MAH end groups. Also, this cluster (or aggregation) formation should be a gradual, not sharp, transition. Furthermore, the degree of the aggregation should be decreased (*not increased*) as the temperature is raised. On the basis of these considerations, we conclude that the transition at 245 °C would not be attributed to the cluster (or aggregation) formation of MAH end groups.

The second reason for the transition at 245 °C might be a morphological transition from lamellae (LAM) to perforated lamellae (PL). The large increase in G' (2 orders of magnitude) was reported during the transition from LAM to PL microdomains,[24] which is consistent with the result in Figure 1. Also, a slight decrease (5−9%) in the microdomain spacing was reported during the transition from LAM to PL,[24,25] which is also in an agreement with the SAXS and TEM results as shown in Figures 3 and 4. Hajduk et al. observed long-lived metastable perforated layer structures (PL) during the transition from LAM to gyroid (G) microdomains, whereas PL was not detected during the transition from G to LAM.[24] Register and co-workers reported thermally reversible transition behaviors in PS-*block*-poly(ethylene-*co*-propylene) copolymers between LAM and PL as well as between PL and CYL.[25,26] During gradual temperature raise, LAM and PL structures coexisted in a wide temperature range between 220 and 260 °C.[25] On the repeated jumping and cooling of the temperature, the transition was remarkably rapid so that the reversible transitions were stabilized within 1 min. The result given in Figure 1b suggests that the reversible transition in this study was also finished within 1 min in a very narrow range of temperature. The fast reversible nature of the transition might be a reason that we could not observe PL in TEM study.

However, there remain some questions regarding the morphological transition from LAM to PL at higher temperatures. Is it possible that SBM66-MAH having symmetric composition could exhibit PL microdomains? PL microdomains have not been reported in block copolymers with symmetric composition (namely, the volume fraction of one of the block is very close to 0.5).[24−26] Also, the addition of single MAH group in SBM66-MAH does not change the volume fraction, since the volume fraction of MAH in SBM66-MAH is just 0.015. At this stage, we do not have any definite explanation for the transition. Another question is why the single MAH end group among four different end groups can effectively change the microdomain morphology. It might be possible that other SBMs with end-functional COOH, diE, and H groups exhibit this transition at very high temperatures (of course, higher than the thermal degradation temperature (∼300 °C)). If this is the case, the transition should be originated from the change in the interaction parameter between PS and PnBMA by the addition of functional groups, as described in the previous study.[9] This argument might be resolved by adding proper solvents with high boiling temperature because the LDOT of neat SBM was judiciously controlled by adjusting the solvent selectivity.[27] This investigation seems to be beyond the scope of this paper and remains as a future study.

In summary, we have observed that the end-functionalized symmetric PS-*b*-PnBMA with MAH exhibited an unexpected thermoreversible transition occurring at a temperature higher than the LDOT. The transition was very fast and induced a large increase in G'. Although a morphological transition between LAM and PL microdomains might be a plausible explanation, the definite origin of this transition is not clear at the current stage.

Acknowledgment. This work was supported by the Creative Research Initiative Program supported by the Korea Science and Engineering Foundation (KOSEF). Small-angle X-ray scattering (4C1 and 4C2) was performed at PLS beamline supported by POSCO and KOSEF. U.J. is thankful for KOSEF grant (No. R01-2007-001-11281-0) funded by MOST. H.J. is grateful to the New Energy and Industrial Technology Development Organization (NEDO) for support through a Japanese National Project "Nano Structured Polymer Project".

Supporting Information Available: Full movies of 3D TEMT for SBM66-MAH annealed at two different temperatures (230 and 260 °C). This material is available free of charge via the Internet at http://pubs.acs.org.

References and Notes

(1) Jalbert, C. J.; Koberstein, J. T.; Yilgor, I.; Gallagher, P.; Krukonis, V. *Macromolecules* **1993**, *26*, 3069.
(2) Fleischer, C. A.; Morales, A. R.; Koberstein, J. T. *Macromolecules* **1994**, *27*, 379.
(3) Elman, J. F.; Johs, B. D.; Long, T. E.; Koberstein, J. T. *Macromolecules* **1994**, *27*, 5341.
(4) Bailey, T. S.; Pham, H. D.; Bates, F. S. *Macromolecules* **2001**, *34*, 6994.
(5) Bailey, T. S.; Hardy, C. M.; Epps, T. H.; Bates, F. S. *Macromolecules* **2002**, *35*, 7007.
(6) Choi, S.; Han, C. D. *Macromolecules* **2003**, *36*, 6220.
(7) Floudas, G.; Pispas, S.; Hadjichristidis, N.; Pakula, T. *Macromol. Chem. Phys.* **2001**, *202*, 1488.
(8) Schacht, P. A.; Koberstein, J. T. *Polymer* **2002**, *43*, 6527.
(9) Jeong, J.; Ryu, D. Y.; Kim, J. K. *Macromolecules* **2003**, *36*, 8913.
(10) Russell, T. P.; Karis, T. E.; Gallot, Y.; Mayes, A. M. *Nature (London)* **1994**, *368*, 729.
(11) Ruzette, A. V. G.; Baerjee, P.; Mayes, A. M.; Pollard, M.; Russell, T. P.; Jerome, R.; Slawecki, T.; Hjelm, R.; Thiyagarajan, P. *Macromolecules* **1998**, *31*, 8509.
(12) Ruzette, A. V. G.; Mayes, A. M.; Pollard, M.; Russell, T. P.; Hammouda, B. *Macromolecules* **2003**, *36*, 3351.
(13) Ryu, D. Y.; Jeong, U.; Lee, D. H.; Kim, J.; Youn, H. W.; Kim, J. K. *Macromolecules* **2003**, *36*, 2894.
(14) Bolze, J.; Kim, J.; Huang, J.; Rah, S.; Youn, H. S.; Lee, B.; Shin, T. J.; Ree, M. *Macromol. Res.* **2002**, *10*, 2.
(15) Kaneko, T.; Nishioka, H.; Nishi, T.; Jinnai, H. *J. Electron Microsc.* **2005**, *54*, 437.
(16) Jinnai, H.; Nishikawa, Y.; Ikehara, T.; Nishi, T. *Adv. Polym. Sci.* **2004**, *170*, 115.
(17) Bates, F. S.; Rosadale, J. H.; Fredrickson, G. H. *J. Chem. Phys.* **1990**, *92*, 6255.
(18) Han, C. D.; Kim, J.; Kim, J. K. *Macromolecules* **1989**, *22*, 383. Han, C. D.; Baek, D. M.; Kim, J. K. *Macromolecules* **1990**, *23*, 561.
(19) Han, C. D.; Baek, D. M.; Kim, J. K.; Ogawa, T.; Hashimoto, T. *Macromolecules* **1995**, *28*, 5043.
(20) Kim, H. J.; Kim, S. B.; Kim, J. K.; Jung, Y. M.; Ryu, D. Y.; Lavery, K. A.; Russell, T. P. *Macromolecules* **2006**, *39*, 408.
(21) Kim, H. J.; Kim, S. B.; Kim, J. K.; Jung, Y. M. *J. Phys. Chem. B* **2006**, *110*, 23123.
(22) Shin, H. S.; Jung, Y. M.; Lee, J.; Chang, T.; Ozaki, Y.; Kim, S. B. *Langmuir* **2002**, *18*, 5523.
(23) Jung, Y. M.; Shin, H. S.; Czarnik-Matusewicz, B.; Noda, I.; Kim, S. B. *Appl. Spectrosc.* **2002**, *56*, 1568.
(24) Hajduk, D. A.; Takenouchi, H.; Hillmyer, M. A.; Bates, F. S.; Vigild, M. E.; Almdal, K. *Macromolecules* **1997**, *30*, 3788.
(25) Loo, Y.-L.; Register, R. A.; Adamson, D. H.; Ryan, A. J. *Macromolecules* **2005**, *38*, 4847.
(26) Lai, C.; Loo, Y.-L.; Register, R. A.; Adamson, D. H. *Macromolecules* **2005**, *38*, 7098.
(27) Li, C.; Lee, D. H.; Kim, J. K.; Ryu, D. Y.; Russell, T. P. *Macromolecules* **2006**, *39*, 5926.

MA0712899